Osmotic pressure characterization of glycosaminoglycans using full-atomistic molecular models

Alejandro Pando Corresp., [1] , **Federica Rigoldi** [2] , **Simone Vesentini** [2]

[1] Center for Biomedical Engineering, Brown University, Division of Hematology and Oncology, Rhode Island Hospital, Providence, RI, United States
[2] Dipartimento di Elettronica, Informazione e Bioingegneria, Politecnico di Milano, Piazza Leonardo da Vinci, Milan, Italy

Corresponding Author: Alejandro Pando
Email address: alejandro_pando@brown.edu

The osmotic pressure of chondroitin sulfate glycosaminoglycans (CS-GAGs) in a simulated physiological environment of articular cartilage is thoroughly examined in silico using full atomistic models. The effects of chemical and physical properties were investigated to elucidate the molecular origins of cartilage biomechanical behavior providing single-atomistic resolution analyses which would not be attainable with in vivo or in in vitro techniques. CS-GAG chains exhibit plastic deformation behavior under compressive load in the extracellular matrix (ECM) and osmotic pressure is the main contributor in balancing external pressures. This study focuses on quantitatively expressing this contribution. Molecular dynamics was used to imitate the physiological environment experienced by GAGs inside articular cartilage by simulating a semipermeable membrane acting on the full atomistic chains during compression. To this end, a variety of validation techniques, pre-simulation tasks, and comparisons were conducted to validate the test methodology. CS-GAGs with varying lengths and sulfation positions underwent simulation under varying molar concentrations. Sulfation positioning is found to have negligible influence on GAG osmotic pressure behavior; attributed to the small distance between the position of 4- and 6- sulfation relative to the intermolecular spacing between the CS chains. However, differences between sulfated and unsulfated chains did have a significant influence on osmotic pressure. Length of disaccharides was also found to have a significant contribution to osmotic pressure. Measurements are comparable to previous coarse grained studies and experimental data.

Title: Osmotic Pressure Characterization of Glycosaminoglycans Using Full-Atomistic Molecular Models

Authors: Alejandro Pando, M.S. (1), Federica Rigoldi (2), Simone Vesentini, Ph. D (2)

Affiliations:
(1) Center for Biomedical Engineering, Brown University, Division of Hematology and Oncology, Rhode Island hospital, Providence, RI, 02906, USA
(2) Dipartimento di Elettronica, Informazione e Bioingegneria, Politecnico di Milano, Piazza Leonardo da Vinci, 32, 20133 Milan, Italy

Corresponding Author:
Prof. Simone Vesentini
Dipartimento di Elettronica, Informazione e Bioingegneria (DEIB) Sezione di Bioingegneria
Politecnico di Milano
Piazza Leonardo da Vinci 32 - 20133 Milano, Italy
Tel: +39 02 2399-3480; Fax: -3360;
website: www.biomech.polimi.it
simone.vesentini@polimi.it

Abstract Word Count: 228

Text Word Count: 3856

Tables: 0

Figures: 3

Short Title: Osmotic Pressure Characterization of Glycosaminoglycans using Full-Atomistic Molecular Models

Keywords: Glycosaminoglycans, Molecular Dynamics, Osmotic Pressure, Collagen, Aggrecan

ABSTRACT

The osmotic pressure of chondroitin sulfate glycosaminoglycan's (CS-GAGs) in a simulated physiological environment of articular cartilage is thoroughly examined *in silico* using full atomistic models. The effects of chemical and physical properties were investigated to elucidate the molecular origins of cartilage biomechanical behavior providing single-atomistic resolution analyses which would not be attainable with *in vivo* or in *in vitro* techniques. CS-GAG chains exhibit plastic deformation behavior under compressive load in the extracellular matrix (ECM) and osmotic pressure is the main contributor in balancing external pressures. This study focuses on quantitatively expressing this contribution. Molecular dynamics was used to imitate the physiological environment experienced by GAGs inside articular cartilage by simulating a semipermeable membrane acting on the full atomistic chains during compression. To this end, a variety of validation techniques, pre-simulation tasks, and comparisons were conducted to validate the test methodology. CS-GAGs with varying lengths and sulfation positions underwent simulation under varying molar concentrations. Sulfation positioning is found to have negligible influence on GAG osmotic pressure behavior; attributed to the small distance between the position of 4- and 6- sulfation relative to the intermolecular spacing between the CS chains. However, differences between sulfated and unsulfated chains did have a significant influence on osmotic pressure. Length of disaccharides was also found to have a significant contribution to osmotic pressure. Measurements are comparable to previous coarse grained studies and experimental data.

INTRODUCTION

Articular cartilage is a hydrated connective tissue which lines the articulating ends of bones, and serves to support mechanical loads, facilitate movements, enable proper joint lubrication, and energy dissipation (Felisbino & Carvalho 1999; Han et al. 2011b; Maroudas 1968). The friction coefficient of an articular cartilage can be as low as 0.005 implying that the frictional force acting tangential to the articular surface may be 200 times smaller than the load transmitted across the joint(Soderberg 1986). During joint motion, cartilage can withstand compressive strains of 10–40%, while sustaining a complex combination of compressive, shear, and tensile stresses up to 20 MPa (Ateshian 2007; Bathe et al. 2005b; Van de Velde et al. 2009). As a result of injury or disease, articular cartilage frequently incurs damage but has limited ability to regenerate (Steinert et al. 2007). In fact, articular cartilage is avascular, hence resident cells (chondrocytes) do not migrate to the lesion, and a production of a tissue with poor properties occurs. The result is typically a suboptimal self-repairing mechanism: the biochemical and mechanical properties of the regenerated cartilage do not equal those of the native one. The gradual failure of the regenerated tissue's load-bearing capability and its subsequent erosion, makes osteoarthritis (OA), one of the ten most disabling diseases in developed countries(Lorenz & Richter 2006). OA refers to a chronic condition characterized by the breakdown of the joint's cartilage where the bones cause stiffness, pain and loss of movement in the joint.

In the past decades, surgical strategies to repair damaged cartilage have been directed towards the use of mechanical penetration of the subchondral bone to disrupt the vasculature and marrow or transplantation of tissues(Steinert et al. 2007). The result is a large clot that fills the defect and enables the natural repair response to form fibrocartilage repair tissue, which is suboptimal to normal cartilage in terms of mechanical properties(Sarzi-Puttini et al. 2005).

Recently, Tissue Engineering (TE) has demonstrated promise for providing more effective alternatives to the above-mentioned solutions. In particular, with its low cellularity and avascular matrix, cartilage has been considered a good candidate for TE because of the lesser demand for metabolite transport and the potentially lower risk of implant rejection by the immune system(Ateshian 2007). Two key disadvantages still face this cell-based therapy: limited number of chondrocytes obtained from biopsy and unmatched mechanical properties of the scaffold(Chung & Burdick 2008). The lack of efficient treatment strategies for cartilage defects has motivated attempts to engineer cartilage constructs *in vitro*. However, none of the current strategies have generated long lasting cartilage replacement tissue that meets the functional demands placed upon this tissue *in vivo* with respect to quality, stability, and integration(Lorenz & Richter 2006; Steinert et al. 2007).

The complex behavior of this tissue resides in the molecular features of the cartilage extracellular matrix (ECM). The cartilage ECM is an intricate network of macromolecules composed mainly of two components defining its mechano-physical properties: the collagenous network, responsible for the tensile strength of the cartilage matrix, and the proteoglycans (PGs), responsible for the osmotic swelling and the elastic properties of the cartilage tissue (Figure 1)(Ateshian 2007; Han et al. 2011b; Hardingham 1981). The primary constituent of the articular cartilage matrix is type II collagen, comprising 80% to 90% of the collagen content. The predominant PG found in articular cartilage is aggrecan, comprising 30-35% of the tissue dry weight together with hyaluronic acid, and it is the primary determinant of cartilage's compressive mechanical properties(Nap & Szleifer 2008).

Aggrecan is a modular PG with multiple functional domains(Dudhia 2005). It's core protein consists of a short interglobular domain, and a long glycosaminoglycan (GAG) attachment

region, which consists of keratan sulfate (KS) and chondroitin sulfate (CS). An aggrecan molecule contains about 100 chondroitin sulfate glycosaminoglycan (CS-GAG) chains covalently bound to a core protein, each having 20–60 disaccharides (N-acetyl-galactosamine and glucuronic acid) that are closely spaced (1–4nm), negatively charged, and possess one carboxylic group and one sulfonic group that varies in location(Dudhia 2005; J. Seog et al. 2002; Nap & Szleifer 2008). The most common scenario involves extensively substituted CS-GAGs with sulfate esters at carbons 4 or 6 of the hexosamine residues(Hardingham 1981; J. Seog et al. 2002). Chondroitin-6-sulfate (CS-6) comprises about 93.3% of the overall CS-GAG chains present in articular cartilage(Lauder et al. 2000). It is generally believed that the functional properties of aggrecans are a direct result of their brush-like structure that ensures dense packing of functional groups along the backbone. The remarkable lubricating effect of such macromolecules is ascribed to interchain repulsion, which leads to the incorporation of large quantities of solvent(Entrialgo-Castaño et al. 2008; Gautieri et al. 2010; Paritosh et al. 2017).

The characteristic bottle-brush structure of the aggrecan is crucial to its behavior: the hydrophilic sugars immobilize large amounts of water within the contact region, while the backbone interconnects to other bottlebrushes(Nap & Szleifer 2008). The interplay of these effects imparts unique biomechanical properties to the tissue, namely a low coefficient of sliding friction even under substantial compressive loads. The relationship between PG aggregates and interstitial fluid provides compressive resilience to cartilage through negative electrostatic repulsion forces(Guterl et al. 2010; Hardingham 1981). The high concentration of GAGs in cartilage generates, in equilibrium, a hydrating osmotic swelling pressure that is opposed by tensile stresses in the surrounding elastic collagen network(Lorenz & Richter 2006). Negatively charged GAG chains contribute to resisting compressive loads on cartilage by interacting with electrolytes in the interstitial fluid to produce a Donnan osmotic pressure relative to the external bathing solution of the tissue, creating an internal pressure that swells the tissue(Chahine et al. 2005; Cheng & Pinsky 2013). The pressure caused by the CS-GAGs prompts cartilage to swell acting as a prestress and enhances the tissue's ability to bear load. Previous studies have shown that this pressure ranges from 0.02 to 2.0 MPa(Ateshian et al. 2004; Lauder et al. 2000). Interestingly, sulfation type (4- versus 6-sulfation of N-acetyl-D-galactosamine in CS), sulfation pattern (statistical distribution of sulfates in CS), molecular weight of CS, and spacing between

CS branch points on the core protein of aggrecan vary significantly with anatomical site, depth within the cartilage layer, age and disease(Dudhia 2005). The osmotic pressure is directly dependent on the fixed charge density of its PGs and kinematic analysis provides the relationship between fixed charge densities and compressive strain(Ateshian et al. 2004; Lai et al. 1991; Narmoneva et al. 2001).

This study implements an investigation of nanoscale compressive properties of CS-GAG chains mimicking physiological conditions, to elucidate the molecular origins of the cartilage biomechanical the relationship between CS-GAGs and osmotic pressure. We developed an in-silico physiological system to replicate the ECM in articular cartilage under joint motion for PGs and sulfated PGs of varying lengths. Previous theoretical studies have examined uncharged macromolecules, featureless GAGs, rigid coarse grained GAGs, and solvent molecules represented by featureless continuums; discounting necessary forces and internal degrees of freedom(Basser & Grodzinsky 1993; Bathe et al. 2005a; Bathe et al. 2005b; Chahine et al. 2005; Urban et al. 1979). The model used in this study is an all-atomic representation of the disaccharide building blocks of GAGs that enables the simulation of physiologically relevant system sizes while retaining the underlying chemical identity of the sugars behavior and providing single-atom resolution which otherwise would not be attainable with experimental techniques. All internal degrees of freedom including bond lengths, valence angles, bond angle bends, bond stretches and torsional angles have the flexibility to respond as they naturally would in normal physiological conditions and the *in-silico* approach allows one to achieve computational tractability. It is of primary interest to gain comprehensive understanding of the molecular relationships of the properties of CS-GAGs and PGs due to their important contribution in TE and biomaterial applications. We demonstrate that the model is directly applicable to the computation of CS-GAG osmotic pressure, and use it to mechanistically investigate the CS-GAG chemical composition osmotic pressure relationship.

METHODS

Model generation: To study the pressure of CS-GAG supramolecular change under compressive physiological environments, we generate fully atomistic models of CS-GAGs in a water

environment with varying ion concentration and chain length. The molecular model construction and molecular dynamics (MD) simulations were performed using NAMD software and CHARMM force field (CHARMM PARAM 36). This force field is robust and widely applicable for the modeling of biomolecular systems consisting of any combination of nucleic acids, proteins, lipids, carbohydrates, and/or small molecules(Guvench et al. 2011). A modified version of the TIP3P model was used to represent water and the SHAKE algorithm was applied to constrain covalent bonds between hydrogens and covalently bound atoms to their equilibrium values(Durell et al. 1994; Jorgensen et al. 1983; Ryckaert et al. 1977). The SHAKE algorithm also kept water molecules rigid(Durell et al. 1994; Jorgensen et al. 1983; Ryckaert et al. 1977). Certain characteristics were modified and called upon by NAMD to account for CS including sulfation, length, and data acquisition parameters. Simulations were performed via NAMD combined with the visualization platform VMD (Humphrey et al. 1996; Phillips et al. 2005).

In the present work, different full atomistic model chains of varying disaccharide lengths account for the effect of the chain length on the osmotic behavior of the solution. The disaccharide chains were modeled starting with alternating sugars (N-acetylgalactosamine and glucuronic acid). Mass of a disaccharide is specified at 457 Dalton/disaccharide according to previous studies(Han et al. 2011a). The periodic box complex was solvated with ≈10,000 TIP3P water molecules and the ionic strength was varied with the addition of Cl^- and Na^+ ions. Ions were included using VMD's autoionize plugin to neutralize the net electric charge of the system (a necessary requirement for simulations with periodic boundary conditions) and to mimic the ionic strength of the solvent that surrounds the protein. CS-GAG chains were placed 2 nm apart from each other to simulate physiological conditions (Song 2010). Bulk solvation energy of the system was based on a previous experiment involving coarse grained CS models (Bathe et al. 2005a; Bathe et al. 2005b). Initial physiological ionic strength of .15 M NaCl was applied and increased to .80 M NaCl.

Finally, we generated a semipermeable membrane and a perpendicular force constant of .1 kcal/mol-Angstrom was applied to the CS-GAG chains parallel to the z-axis to simulate compression imitating the physiological forces experienced at the joint. A perpendicular force

constant of .1 kcal/mol-Angstrom was chosen to increase acquisition of data points from the contact moment; effectively allowing the membrane to experience greater contact with CS-GAG chains while allowing simulation output of contact moment data. Validation techniques of the semi-permeable membrane were conducted based on prior literature and methods (Gautieri et al. 2010; Luo & Roux 2009). Briefly, the osmotic pressure of NaCl and KCl aqueous solution were calculated over a range of concentrations (5, 1, 2, 3, 4, and 5 M) and compared with prior studies and experimental values (Luo & Roux 2009; Robinson 2002). The virtual membrane constrained the CS-GAG chains while leaving ions and water molecules unconstrained. The sulfated CS-GAG chains were in a solvation box with a total atom number varying from ≈ 11,000 atoms to ≈ 22,000 atoms (for highly solvated systems) mimicking physiological conditions that the chains undergo.

Model Equilibration: Fully atomistic simulations are carried out using NAMD. The initial geometries of the models are refined following a procedure previously implemented and tested which consists of MD calculations at different temperature and groups to obtain chain redistribution within the periodic cell(Entrialgo-Castano et al. 2006; Entrialgo-Castaño et al. 2008; Gautieri et al. 2010; Gautieri et al. 2011; Ionita et al. 2017). The molecular models were minimized and equilibrated using the NAMD code under constant pressure and temperature (NPT) conditions in order to relax the volume of the periodic box(Nelson et al. 1996). Preliminary minimization and NPT equilibration were set at constant temperature with Langevin dynamics and periodic boundary conditions. The temperature was set to 300 K and the pressure to 1 atm, while utilizing a time step of 2 fs, rigid bonds, and particle-mesh Ewald long-range electrostatics. MD simulations are visually displayed in VMD. The particle-mesh Ewald summation (PME) method is applied to describe electrostatic interactions and Langevin Dynamics was used as a way of controlling temperature. Nonbonding interactions were computed using a cutoff for neighbor chains at 1 nm, with a switching function between 1.2 nm for van der Waals interactions. Potential energy, temperature, pressure and density were validated for stable values after each step of the equilibration procedure. Timestep (2 fs) was optimized for targeted information and interpretation. Convergence of the root mean square deviation (RMSD) was utilized to monitor the stability of the system. Following MD

simulations, all analyses were conducted using the VMD software package (Humphrey et al. 1996).

In silico System Testing: To assess the mechanical properties of the CS-GAG atomistic chain models, we performed MD simulations with increasing constant mechanical stress along the perpendicular axis from dual sides, while maintaining the other axes constant. Four CS-GAG chains were placed in the periodic box at 2 nm apart from each other because this is the most accurate spacing of the chains observed (Song 2010). The mechanical load implemented here reflects that used for mechanical testing in experimental studies (Rodríguez-Carvajal et al. 2017). In this system, it is important to use as large a timestep as possible to sample phase space rapidly and save on computer expense. The size of the model and its fully atomistic characteristics are large and computationally demanding requiring 6-8 hours per nanosecond on 32 CPUs on a parallel machine.

RESULTS AND DISCUSSION

In this study, we apply a fully atomistic representation of CS-GAGs in the cartilage ECM environment using MD simulations, replicating joint biomechanical movement and capturing the biochemical features of PG molecules to describe mechanical behavior at the molecular level. CS is the major sulfated GAG in the matrix of joint tissues and is characterized by repetitive sulfated disaccharide units, β-d-glucuronic acid (GlcUA) and 2-acetamido-2-deoxy-β-d-acetylgalactose(GalNAc), joined by β (1→4) and β (1→3) linkages (Figure 2c)(Cilpa et al. 2010; J. Seog et al. 2002). A typical chondroitin chain can have over a hundred individual sugars each of which can be unsulfated or sulfated at the carbon -4 or -6 positions (Jones et al. 2003). CS-GAG chains are negatively charged and contribute to resisting compressive loads on cartilage during mechanical loading, and understanding the effects changes in CS-GAG chemical composition impose on mechanical properties was investigated. The system environment was replicated by building different disaccharide length chondroitin or CS chains with different positions of sulfation, and placing them in an ionized solvation box (Figure 2a). GAG separation distance between two neighboring CS-GAG molecular chains was approximated to be 2nm from previous investigations (Figure 2b)(Song 2010). To account for age, disease and other underlying

factors that may influence the character of the articular cartilage matrix, the molar concentrations of the environment was varied. A semipermeable membrane was constructed *in silico* that compresses the CS-GAG chains while leaving the water and sodium ions to roam freely (Figure 2d and 2e). This was imitated for different concentrations to account for the transient environment that articular cartilage experiences. CS-GAG chain parameters rely on a previous study by Cilpa G and authors, who combine the use of experimental techniques and methods of Quantum mechanics to estimate the individual values of CS-6 disaccharides(Cilpa et al. 2010). The conformations around the glycosidic linkages are described by two sets of torsional angles ψ/ϕ. The MD simulations used in the present study are based on the classical mechanic's theory, neglecting quantum mechanics effects.

Previous investigations have shown that above 1 M NaCl the osmotic pressure changes negligibly, suggesting that Donnan osmotic pressure is negligible above this threshold (Chahine et al. 2005). Osmotic pressure equilibrium in PGs is achieved through both electrostatic and van der Waals contributions. The electrostatic components have been previously described by Donnan pressure and microstructural modeling of GAG molecules(Basser et al. 1998; Buschmann & Grodzinsky 1995; Lai et al. 1991; Maroudas 1968). Electrostatic contributions to osmotic pressure are dependent on electrolyte concentration according to Donnan's law and because excess ions act as a shield for electrostatic repulsion of GAG chains, Donnan charge contribution becomes negligible at high concentrations in agreement with previous studies(Basser & Grodzinsky 1993; Buschmann & Grodzinsky 1995; Chahine et al. 2005).

Data showed similar results between four sulfated and six sulfated CS-GAG chains, suggesting that sulfation position is a negligible factor in osmotic pressure determination. Osmotic pressure in Donnan equilibrium is dependent on the number of fixed charges which can partly explain why CS4 and CS6 behave similar. (Figure 3a). There was an increase in osmotic pressure when sulfation was present compared to unsulfated. This is partly attributed to the molecular weight and polarity exhibited by a sulfation molecule along with an increase in the number of fixed charges (Figure 3a). To further characterize physiological CS-GAG behavior in its environment, various lengths (2, 4 and 8-monomers) of monosaccharide chains were examined. Length of CS-GAG chains were increased and doubled (Figure 3b). Varied lengths of chains were chosen to

investigate a relationship between length and osmotic pressure that can be applied to analytically expand on the biomechanical behavior experienced within a physiological environment. The chains were setup at equal distances (2nm) from each other to simulate physiological conditions according to previous investigations and from the outer solvation box(Song 2010). Ionic strengths and water concentrations were adjusted accordingly to control for varying length of chains. Results indicated that length of chains positively correlated with osmotic pressure, demonstrating that smaller monomer chains had a smaller osmotic pressure then those with more repeating units (Figure 3b). Molar concentration and osmotic pressure were also positively correlated, with a greater molar concentration leading to a higher osmotic pressure in all cases (Figure 3c). GAG sulfation played a role in osmotic pressure as well, with sulfated chains of the same length displaying higher osmotic pressure than their unsulfated counterparts in all cases (Figure 3c). However, chain length was the primary determinant of osmotic pressure and sulfation state played a small role (Figure 3a and b). Results indicate that osmotic pressure is predominantly affected by intermolecular carboxylate-sulfate and carboxylate-carboxylate interactions (Figure 3c). Previous studies have investigated the subject of varying sulfation within a single chain of CS-GAG and our results compliment theirs, further suggesting that osmotic pressure is insensitive to these variations(Bathe et al. 2005b; Luo & Roux 2009).

CONCLUSION

The main surveying techniques for CS characterization and properties are Nuclear Magnetic Resonance and X-ray crystallography. Molecular modeling simulations have shown to provide an accurate representation of results compared to experimental techniques using NMR spectroscopy and x-ray crystallography(Brooks et al. 2009; Sattelle et al. 2010). Although NMR spectroscopy and x-ray crystallography are beneficial and provide valuable information, they provide only partial information while *in silico* simulations provide more detailed characteristics(Sattelle et al. 2010). This is due to the construction of the GAG chains and their inability to be confined to a strictly stable confirmation but instead having multiple structures. Previous investigations using coarse grained models have approximated and generated pretabulated potentials for GAG chain characteristics not fully representing the supramolecular characteristics of GAG's. These models do not account for internal degrees of freedom including

bond lengths, valence angles, and torsional angles. The methods applied here apply a full atomistic model with all internal degrees of freedom including bond lengths, valence angles, bond stretches, and torsional angles having the flexibility to respond as they naturally would in a physiological environment providing motion and force relationships that are not possible in the coarse-grained bodies used in previous studies(Bathe et al. 2005a; Bathe et al. 2005b; Brooks et al. 2009; Ehrlich et al. 1998; Hummer & Kevrekidis 2003). Similarly, previous studies have investigated osmotic properties using models where solvent molecules are represented by a featureless continuum(Luo & Roux 2009), the use of equilibrium dialysis(Basser et al. 1998; Ehrlich et al. 1998; Urban et al. 1979), or sedimentation equilibrium(Williams & Comper 1990). Many of these methods are measured through indirect chemical equilibration measurements, where the charge of the CS-GAGs are not considered and compared to uncharged macromolecules that do not consider all characteristics such as an increase in temperature(Basser et al. 1998; Chahine et al. 2005; Ehrlich et al. 1998; Urban et al. 1979).

Our model, applies an infinite wall to represent the effect of ideal semipermeable membranes, separating a high concentration region from a pure water region. The virtual membrane compresses the chains while allowing water to pass freely, permitting an equalization of their chemical potential throughout the entire system. The mean force per unit area exerted on the ions by the virtual walls during the simulations can be directly related to the osmotic pressure. This method bares similarities and adapts those developed by Rout and Murad where the osmotic pressure was calculated from the mean force of a membrane in an ion solution(Luo & Roux 2009; Murad & Powles 1993; Murad et al. 1995; Paritosh et al. 2017). Our model allows for the capture of major structural features of CS-GAG and the mechanical behavior at different hierarchical levels and different levels of mechanical deformation.

The results of this study are in qualitative agreement with the study of Bathe et al., which examined the osmotic pressure of coarse grained GAG chains(Bathe et al. 2005a; Bathe et al. 2005b). Both studies demonstrate that the osmotic pressure of the GAG systems increase with molar concentration. However, quantitatively the measured pressures differ slightly with varying sulfation and disaccharide length and can be attributed to the full atomistic model implemented. Moreover, previous studies were based on an approximate molecular model that contains numerous potentially limiting assumption and theories such as the Donnan theory and the

Poisson-Boltzmann theory. Instead this study utilized mechanical loading in the form of a semipermeable membrane biaxial force to directly relate to the osmotic pressure within the articular cartilage environment. The membrane was observed to act as hypothesized and kept stable during the simulation with no extensive deviations, performing its purpose with excellent results. Moreover, our results have shown congruency with previous simple models, while providing significant data dissimilarities that must be further analyzed to more thoroughly understand the characteristics of CS-GAGs.

In conclusion, this study finds that the osmotic pressure of CS-GAG chains measured at physiological environments within articular cartilage increases with molar concentration. As expected, osmotic pressure and molar concentration were positively correlated and chain length had a significant effect on pressure. Past studies have suggested that GAG macromolecules contribute significantly more to the compressive modulus than suggested from Donnan osmotic effects alone. Consistent with prior literature reports measuring properties of cartilage in isotonic and hypertonic salt solutions, we demonstrate that osmotic effects do contribute a significant amount of the compressive modulus in cartilage. The osmotic pressure is attributed mostly to intrinsic effects, not electrostatic forces and pinpoints an important factor in compression/tension within the ECM of the articular cartilage(Bathe et al. 2005a). CS-GAGs are negatively charged, linear polyelectrolytes composed of between 50 and 100 disaccharides that supply energy for the compression cycle. Further examination on chain length and quantum mechanical properties on biomechanical behavior are warranted, however the method applied here are comparable and can be quantitatively applied to explain supplementary behavior.

Acknowledgements

We gratefully acknowledge our funding source (CRISP Atlantis International Program) as well as technical assistance provided by staff at the Politecnico di Milano Biomechanics Lab.

436
437
438
439
440
441
442
443
444
445
446
447
448

449 **References**

450 Ateshian GA. 2007. Artificial cartilage: weaving in three dimensions. *Nat Mater*. England, 89-
451 90.
452 Ateshian GA, Chahine NO, Basalo IM, and Hung CT. 2004. The correspondence between
453 equilibrium biphasic and triphasic material properties in mixture models of articular
454 cartilage. *J Biomech* 37:391-400.
455 Basser PJ, and Grodzinsky AJ. 1993. The Donnan model derived from microstructure. *Biophys*
456 *Chem* 46:57-68.
457 Basser PJ, Schneiderman R, Bank RA, Wachtel E, and Maroudas A. 1998. Mechanical
458 properties of the collagen network in human articular cartilage as measured by osmotic
459 stress technique. *Arch Biochem Biophys* 351:207-219. 10.1006/abbi.1997.0507
460 Bathe M, Rutledge GC, Grodzinsky AJ, and Tidor B. 2005a. A coarse-grained molecular model
461 for glycosaminoglycans: application to chondroitin, chondroitin sulfate, and hyaluronic
462 acid. *Biophys J* 88:3870-3887. 10.1529/biophysj.104.058800
463 Bathe M, Rutledge GC, Grodzinsky AJ, and Tidor B. 2005b. Osmotic Pressure of Aqueous
464 Chondroitin Sulfate Solution: A Molecular Modeling Investigation. *Biophys J*, 2357-
465 2371.

466 Brooks BR, Brooks CL, 3rd, Mackerell AD, Jr., Nilsson L, Petrella RJ, Roux B, Won Y,
467 Archontis G, Bartels C, Boresch S, Caflisch A, Caves L, Cui Q, Dinner AR, Feig M,
468 Fischer S, Gao J, Hodoscek M, Im W, Kuczera K, Lazaridis T, Ma J, Ovchinnikov V,
469 Paci E, Pastor RW, Post CB, Pu JZ, Schaefer M, Tidor B, Venable RM, Woodcock HL,
470 Wu X, Yang W, York DM, and Karplus M. 2009. CHARMM: the biomolecular
471 simulation program. *J Comput Chem* 30:1545-1614. 10.1002/jcc.21287
472 Buschmann MD, and Grodzinsky AJ. 1995. A molecular model of proteoglycan-associated
473 electrostatic forces in cartilage mechanics. *J Biomech Eng* 117:179-192.
474 Chahine NO, Chen FH, Hung CT, and Ateshian GA. 2005. Direct measurement of osmotic
475 pressure of glycosaminoglycan solutions by membrane osmometry at room temperature.
476 *Biophys J* 89:1543-1550. 10.1529/biophysj.104.057315
477 Cheng X, and Pinsky PM. 2013. Mechanisms of self-organization for the collagen fibril lattice in
478 the human cornea. *J R Soc Interface* 10:20130512. 10.1098/rsif.2013.0512
479 Chung C, and Burdick JA. 2008. Engineering Cartilage Tissue. *Adv Drug Deliv Rev* 60:243-262.
480 10.1016/j.addr.2007.08.027
481 Cilpa G, Hyvonen MT, Koivuniemi A, and Riekkola ML. 2010. Atomistic insight into
482 chondroitin-6-sulfate glycosaminoglycan chain through quantum mechanics calculations
483 and molecular dynamics simulation. *J Comput Chem* 31:1670-1680. 10.1002/jcc.21453
484 Dudhia J. 2005. Aggrecan, aging and assembly in articular cartilage. *Cell Mol Life Sci* 62:2241-
485 2256. 10.1007/s00018-005-5217-x
486 Durell SR, Brooks BR, and Ben-Naim A. 1994. Solvent-Induced Forces between Two
487 Hydrophilic Groups. 10.1021/j100059a038
488 Ehrlich S, Wolff N, Schneiderman R, Maroudas A, Parker KH, and Winlove CP. 1998. The
489 osmotic pressure of chondroitin sulphate solutions: experimental measurements and
490 theoretical analysis. *Biorheology* 35:383-397.
491 Entrialgo-Castano M, Lendlein A, and Hofmann D. 2006. Molecular modeling investigations of
492 dry and two water-swollen states of biodegradable polymers. *Advanced engineering*
493 *materials* 8:434-439. eva7837
494 Entrialgo-Castaño M, GKSS Research Center IoPR, Kantstrasse 55, 14513 Teltow, Germany,
495 Salvucci AE, Department of Biological and Environmental Engineering RRH, Cornell
496 University, Ithaca, NY 14853, Lendlein A, GKSS Research Center IoPR, Kantstrasse 55,
497 14513 Teltow, Germany, Hofmann D, GKSS Research Center IoPR, Kantstrasse 55,
498 14513 Teltow, Germany, and GKSS Research Center IoPR, Kantstrasse 55, 14513
499 Teltow, Germany Fax: (+49) 3328 352 452. 2008. An Atomistic Modeling and Quantum
500 Mechanical Approach to the Hydrolytic Degradation of Aliphatic Polyesters.
501 *Macromolecular Symposia* 269:47-64. 10.1002/masy.200850908
502 Felisbino SL, and Carvalho HF. 1999. The epiphyseal cartilage and growth of long bones in
503 Rana catesbeiana. *Tissue Cell* 31:301-307. 10.1054/tice.1999.0036
504 Gautieri A, Ionita M, Silvestri D, Votta E, Vesentini S, Fiore GB, Barbani N, Ciardelli G, and
505 Redaelli A. 2010. Computer-Aided Molecular Modeling and Experimental Validation of
506 Water Permeability Properties in Biosynthetic Materials. info:doi/10.1166/jctn.2010.1482
507 Gautieri A, Vesentini S, Redaelli A, and Buehler MJ. 2011. Hierarchical structure and
508 nanomechanics of collagen microfibrils from the atomistic scale up. *Nano Lett* 11:757-
509 766. 10.1021/nl103943u

510 Guterl CC, Hung CT, and Ateshian GA. 2010. Electrostatic and Non-Electrostatic Contributions
511 of Proteoglycans to the Compressive Equilibrium Modulus of Bovine Articular Cartilage.
512 *J Biomech* 43:1343-1350. 10.1016/j.jbiomech.2010.01.021
513 Guvench O, Mallajosyula SS, Raman EP, Hatcher E, Vanommeslaeghe K, Foster TJ, Francis W.
514 Jamison I, and Alexander D. MacKerell J. 2011. CHARMM Additive All-Atom Force
515 Field for Carbohydrate Derivatives and Its Utility in Polysaccharide and Carbohydrate–
516 Protein Modeling. 10.1021/ct200328p
517 Han E, Chen S, Klisch S, and Sah R. 2011a. Contribution of Proteoglycan Osmotic Swelling
518 Pressure to the Compressive Properties of Articular Cartilage. *Biophys J*, 916-924.
519 Han L, Grodzinsky AJ, and Ortiz C. 2011b. Nanomechanics of the Cartilage Extracellular
520 Matrix. *Annu Rev Mater Res* 41:133-168. 10.1146/annurev-matsci-062910-100431
521 Hardingham T. 1981. Proteoglycans: their structure, interactions and molecular organization in
522 cartilage. *Biochem Soc Trans* 9:489-497.
523 Harvey MJ, Giupponi G, and Fabritiis GD. 2009. ACEMD: Accelerating Biomolecular
524 Dynamics in the Microsecond Time Scale. 10.1021/ct9000685
525 Hummer G, and Kevrekidis IG. 2003. Coarse molecular dynamics of a peptide fragment: Free
526 energy, kinetics, and long-time dynamics computations. *J Chem Phys* 118(23):10762 -
527 10773. 1.1574777
528 Humphrey W, Dalke A, and Schulten K. 1996. VMD: visual molecular dynamics. *J Mol Graph*
529 14:33-38, 27-38.
530 Ionita M, Silvestri D, Gautieri A, Votta E, Ciardelli G, and Redaelli A. 2017. Diffusion of small
531 molecules in bioartificial membranes for clinical use: molecular modelling and laboratory
532 investigation. *Desalination* 200:157-159.
533 J. Seog, D. Dean, A. H. K. Plaas, S. Wong-Palms, A. J. Grodzinsky, ‡ and, and C. Ortiz*. 2002.
534 Direct Measurement of Glycosaminoglycan Intermolecular Interactions via High-
535 Resolution Force Spectroscopy. S0024-9297(01)02162-3
536 Jones LL, Margolis RU, and Tuszynski MH. 2003. The chondroitin sulfate proteoglycans
537 neurocan, brevican, phosphacan, and versican are differentially regulated following
538 spinal cord injury. *Exp Neurol* 182:399-411.
539 Jorgensen WL, Chandrasekhar J, Madura JD, Impey RW, and Klein ML. 1983. Comparison of
540 simple potential functions for simulating liquid water. *The Journal of Chemical Physics*
541 79:926-935. 1.445869
542 Lai WM, Hou JS, and Mow VC. 1991. A triphasic theory for the swelling and deformation
543 behaviors of articular cartilage. *J Biomech Eng* 113:245-258.
544 Lauder RM, Huckerby TN, and Nieduszynski IA. 2000. A fingerprinting method for
545 chondroitin/dermatan sulfate and hyaluronan oligosaccharides. *Glycobiology* 10:393-401.
546 Lorenz H, and Richter W. 2006. Osteoarthritis: cellular and molecular changes in degenerating
547 cartilage. *Prog Histochem Cytochem* 40:135-163. 10.1016/j.proghi.2006.02.003
548 Luo Y, and Roux B. 2009. Simulation of Osmotic Pressure in Concentrated Aqueous Salt
549 Solutions. 10.1021/jz900079w
550 Maroudas A. 1968. Physicochemical properties of cartilage in the light of ion exchange theory.
551 *Biophys J* 8:575-595. 10.1016/s0006-3495(68)86509-9
552 Murad S, and Powles JG. 1993. A computer simulation of the classic experiment on osmosis and
553 osmotic pressure. *Journal of Chemical Physics* 99:7271-7272. doi:10.1063/1.465421

554 Murad S, Powles JG, and Holtz B. 1995. Osmosis and reverse osmosis in solutions: Monte Carlo
555 simulations and van der Waals one-fluid theory. *Molecular Physics* 86:1473-1483.
556 doi:10.1080/00268979500102861
557 Nap RJ, and Szleifer I. 2008. Structure and Interactions of Aggrecans: Statistical
558 Thermodynamic Approach. *Biophys J*, 4570-4583.
559 Narmoneva DA, Wang JY, and Setton LA. 2001. A noncontacting method for material property
560 determination for articular cartilage from osmotic loading. *Biophys J* 81:3066-3076.
561 10.1016/s0006-3495(01)75945-0
562 Nelson MT, Urbana-Champaign UoIa, Humphrey W, Urbana-Champaign UoIa, Gursoy A,
563 Urbana-Champaign UoIa, Dalke A, Urbana-Champaign UoIa, Kale LV,
564 kale@illinois.edu, Computer Science NCfSAN, Beckman Institute for Advanced Science
565 and Technology, Skeel RD, Urbana-Champaign UoIa, Schulten K, schulten@illinois.edu,
566 and Physics BIfASaT, Chemistry, Bioengineering, Micro and Nanotechnology Lab.
567 1996. NAMD: A parallel, object-oriented molecular dynamics program. *International*
568 *Journal of High Performance Computing Applications* 10:251-268.
569 Paritosh F, Chemical Engineering Dept. UoIaC, Chicago, IL 60607, Murad S, and Chemical
570 Engineering Dept. UoIaC, Chicago, IL 60607. 2017. Molecular simulations of osmosis
571 and reverse osmosis in aqueous electrolyte solutions. *AIChE Journal* 42:2984-2986.
572 10.1002/aic.690421026
573 Phillips JC, Braun R, Wang W, Gumbart J, Tajkhorshid E, Villa E, Chipot C, Skeel RD, Kale L,
574 and Schulten K. 2005. Scalable molecular dynamics with NAMD. *J Comput Chem*
575 26:1781-1802. 10.1002/jcc.20289
576 Robinson RA. 2002. Electrolyte solutions / R.A. Robinson, R.H. Stokes. .
577 Rodríguez-Carvajal MA, Centre de Recherches sur les Macromolécules Végétales C, F-38041
578 Grenoble, France, Imberty A, Centre de Recherches sur les Macromolécules Végétales C,
579 F-38041 Grenoble, France, Pérez S, Centre de Recherches sur les Macromolécules
580 Végétales C, F-38041 Grenoble, France, and Centre de Recherches sur les
581 Macromolécules Végétales C, F-38041 Grenoble, France. 2017. Conformational behavior
582 of chondroitin and chondroitin sulfate in relation to their physical properties as inferred
583 by molecular modeling. *Biopolymers* 69:15-28. 10.1002/bip.10304
584 Ryckaert JP, Ciccotti G, and Berendsen HJC. 1977. Numerical integration of the cartesian
585 equations of motion of a system with constraints: molecular dynamics of n-alkanes.
586 *Journal of Computational Physics*. 10.1016/0021-9991(77)90098-5
587 Sarzi-Puttini P, Cimmino MA, Scarpa R, Caporali R, Parazzini F, Zaninelli A, Atzeni F, and
588 Canesi B. 2005. Osteoarthritis: an overview of the disease and its treatment strategies.
589 *Semin Arthritis Rheum* 35:1-10. 10.1016/j.semarthrit.2005.01.013
590 Sattelle BM, Shakeri J, Roberts IS, and Almond A. 2010. A 3D-structural model of unsulfated
591 chondroitin from high-field NMR: 4-sulfation has little effect on backbone conformation.
592 *Carbohydr Res*, 291-302.
593 Soderberg G. 1986. Kinesiology: Application to pathological Motion. *2nd ed Baltimore:*
594 *Williams & Wilkins*.
595 Song F. 2010. Interactions between nearest-neighboring glycosaminoglycan molecules of
596 articular cartilage. *Mol Cell Biomech* 7:13-23.
597 Steinert AF, Ghivizzani SC, Rethwilm A, Tuan RS, Evans CH, and Nöth U. 2007. Major
598 biological obstacles for persistent cell-based regeneration of articular cartilage. *Arthritis*
599 *Res Ther*, 213.

Urban JP, Maroudas A, Bayliss MT, and Dillon J. 1979. Swelling pressures of proteoglycans at the concentrations found in cartilaginous tissues. *Biorheology* 16:447-464.
Van de Velde SK, Bingham JT, Hosseini A, Kozanek M, DeFrate LE, Gill TJ, and Li G. 2009. Increased tibiofemoral cartilage contact deformation in patients with anterior cruciate ligament deficiency. *Arthritis Rheum* 60:3693-3702. 10.1002/art.24965
Williams RP, and Comper WD. 1990. Osmotic flow caused by polyelectrolytes. *Biophys Chem* 36:223-234.

Figure 1: Hierarchical structure of proteoglycan molecules. Bones of a synovial joint are covered by a layer of articular cartilage that lines the epiphyses of the bone. The extracellular matrix (ECM) of articular cartilage consists mainly of proteoglycans (mostly aggrecan) and collagens that respond to tensile and compressive load. Aggrecan has a densely-packed array of highly negatively charged, linear chondroitin sulfate glycosaminoglycan (CS-GAG) chains along its core protein [16, 20]. Aggrecan has a molecular mass >2,500 kDa when combining the core protein (~300 kDa) and the mass of the 100 CS-GAG chains [21,22]. CS-GAGs are composed of between 10 and 50 repeats of the disaccharide (N-acetyl-galactosamine and glucuronic acid) that play an important role in mechanical function, stiffness, and compressive load resistance [14, 22].

Figure 2: Multi-modeling microenvironment framework. **a)** System generated. VMD visualization of TIP3P water molecules (blue) surround the CS-GAG chains (red) generated by NAMD. Positively charged ions (yellow) surround the system. **b)** CS-GAG configuration. Each GAG chain is separated by a distance of 2 nm (Song 2010). **c)** Single chondroitin-4-sulfate chain visualized in VMD software. Carbon atoms (teal), Oxygen atoms (red), Sulfur atoms (yellow), Nitrogen atoms (blue), Hydrogen atoms (white). **d)** Red molecules to the right and left of CS-GAG chains are constructed virtual continuous semipermeable membranes. Semipermeable membranes and CS-GAG's are parallel with z-axis. A perpendicular force is applied to the CS-GAG chains. Water molecules have been removed for visualization purposes. **e)** Multiple compression simulations of CS-GAG chains. Compressed by the semipermeable membrane in the solvent box. Images taken from top view.

Figure 3: Chondroitin Sulfate glycosaminoglycan (CS-GAG) behavior, quantitative comparison with experimental results. The mechanical properties of CS-GAGs are determined by applying an increasing mechanical force (negative pressure) along the chain axis with varying ionic concentration. **a)** Osmotic pressure vs. molar concentration. Trends of CS-GAG sulfation and

sulfation position in molar concentrations on osmotic pressure. Sulfation at the carbon-4 (orange) or carbon-6(blue) position of N-acetylgalactosamine did not significantly differ osmotic pressure. Lack of CS-GAG sulfation (gray) demonstrated decreased osmotic pressure then sulfated counterpart GAGs. Four monomer CS-GAG (Left). Eight monomer CS-GAG (Right) **b)** Average osmotic pressure vs. molar concentration. Graph shows the effect doubling CS-GAG disaccharide length has on osmotic pressure. Basal GAG length (green) and double the basal disaccharide length (blue) **c)** Osmotic pressure and molar concentration trends in CS-GAGs. Chondroitin-6-sulfate and chondroitin-4-sulfate 8 monosaccharide chains demonstrated the highest osmotic pressure for all molar concentrations. Osmotic pressure shows an increased dependence on CS-GAG disaccharide length and on whether sulfation occurred or not. However, it is not significantly influenced by CS-GAG sulfation position. C6S-GAG 8 monomer (blue) C4S-GAG 8 monomer (orange) CS-GAG 8 monomer (gray) C6S-GAG 4 monomer (yellow) C4S-GAG 4 monomer (teal) CS-GAG 4 monomer (green). Statistical error bars are smaller than the symbols.

Figure 1(on next page)

Figure 1

Figure 1: Hierarchical structure of proteoglycan molecules. Bones of a synovial joint are covered by a layer of articular cartilage that lines the epiphyses of the bone. The extracellular matrix (ECM) of articular cartilage consists mainly of proteoglycans (mostly aggrecan) and collagens that respond to tensile and compressive load. Aggrecan has a densely-packed array of highly negatively charged, linear chondroitin sulfate glycosaminoglycan (CS-GAG) chains along its core protein [16, 20]. Aggrecan has a molecular mass >2,500 k Da when combining the core protein (~300 kDa) and the mass of the 100 CS-GAG chains [21,22]. CS-GAGs are composed of between 10 and 50 repeats of the disaccharide (N-acetyl-galactosamine and glucuronic acid) that play an important role in mechanical function, stiffness, and compressive load resistance [14, 22].

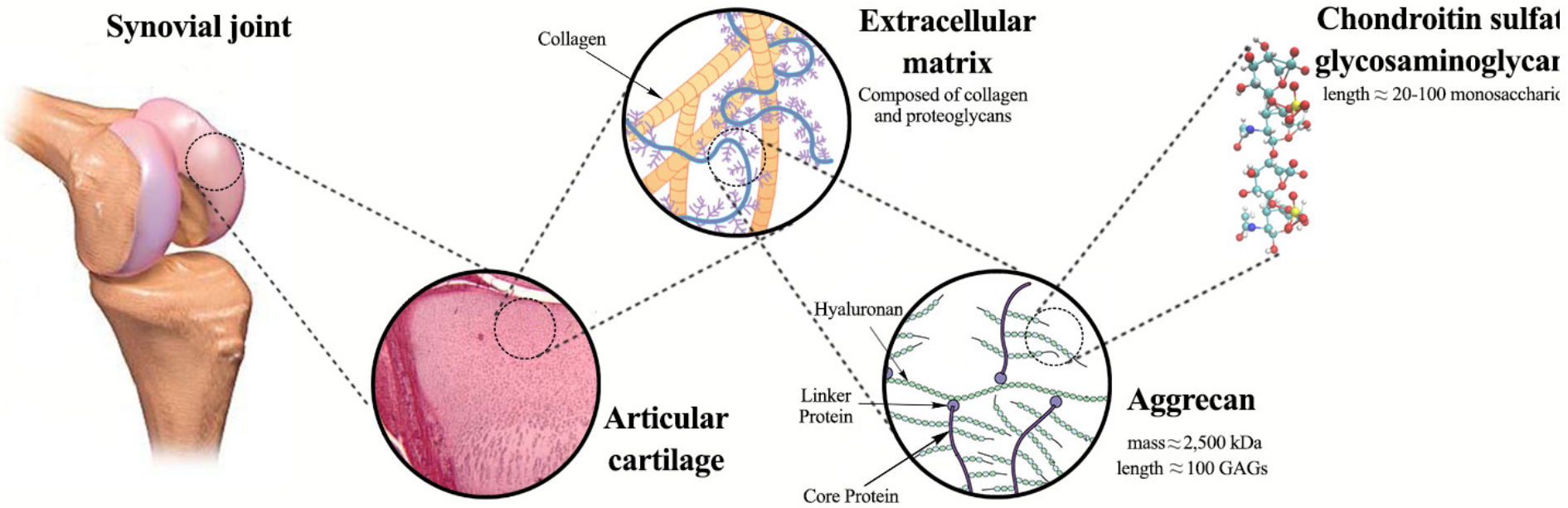

Figure 2(on next page)

Figure 2

Figure 2: Multi-modeling microenvironment framework. **a)** System generated. VMD visualization of TIP3P water molecules (blue) surround the CS-GAG chains (red) generated by NAMD. Positively charged ions (yellow) surround the system. **b)** CS-GAG configuration. Each GAG chain is separated by a distance of 2 nm (Song 2010) . **c)** Single chondroitin-4-sulfate chain visualized in VMD software. Carbon atoms (teal), Oxygen atoms (red), Sulfur atoms (yellow), Nitrogen atoms (blue), Hydrogen atoms (white). **d)** Red molecules to the right and left of CS-GAG chains are constructed virtual continuous semipermeable membranes. Semipermeable membranes and CS-GAG's are parallel with z-axis. A perpendicular force is applied to the CS-GAG chains. Water molecules have been removed for visualization purposes. **e)** Multiple compression simulations of CS-GAG chains. Compressed by the semipermeable membrane in the solvent box. Images taken from top view.

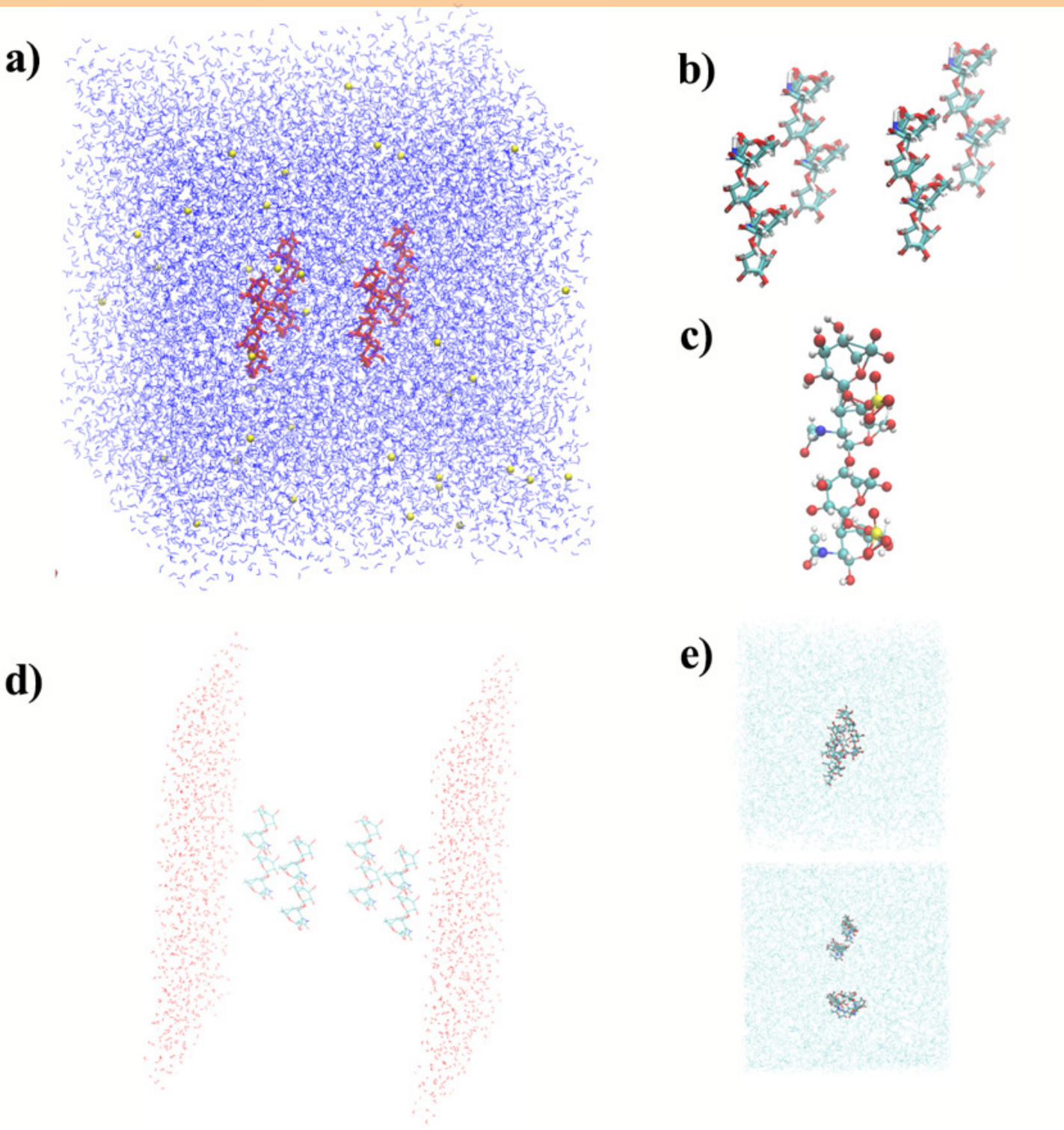

PeerJ Preprints | https://doi.org/10.7287/peerj.preprints.3063v1 | CC BY 4.0 Open Access | rec: 1 Jul 2017, publ: 1 Jul 2017

Figure 3(on next page)

Figure 3

Figure 3: Chondroitin Sulfate glycosaminoglycan (CS-GAG) behavior, quantitative comparison with experimental results. The mechanical properties of CS-GAGs are determined by applying an increasing mechanical force (negative pressure) along the chain axis with varying ionic concentration. **a)** Osmotic pressure vs. molar concentration. Trends of CS-GAG sulfation and sulfation position in molar concentrations on osmotic pressure. Sulfation at the carbon-4 (orange) or carbon-6(blue) position of N-acetylgalactosamine did not significantly differ osmotic pressure. Lack of CS-GAG sulfation (gray) demonstrated decreased osmotic pressure then sulfated counterpart GAGs. Four monomer CS-GAG (Left). Eight monomer CS-GAG (Right) **b)** Average osmotic pressure vs. molar concentration. Graph shows the effect doubling CS-GAG disaccharide length has on osmotic pressure. Basal GAG length (green) and double the basal disaccharide length (blue) **c)** Osmotic pressure and molar concentration trends in CS-GAGs. Chondroitin-6-sulfate and chondroitin-4-sulfate 8 monosaccharide chains demonstrated the highest osmotic pressure for all molar concentrations. Osmotic pressure shows an increased dependence on CS-GAG disaccharide length and on whether sulfation occurred or not. However, it is not significantly influenced by CS-GAG sulfation position. C6S-GAG 8 monomer (blue) C4S-GAG 8 monomer (orange) CS-GAG 8 monomer (gray) C6S-GAG 4 monomer (yellow) C4S-GAG 4 monomer (teal) CS-GAG 4 monomer (green). Statistical error bars are smaller than the symbols.

a)

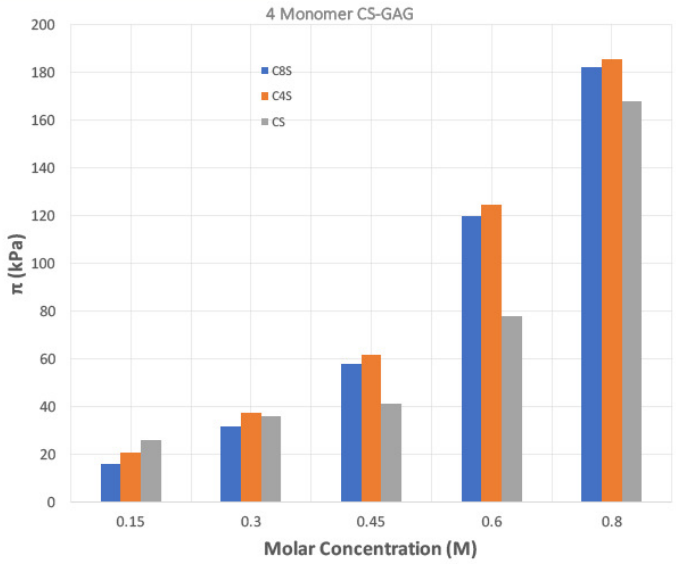

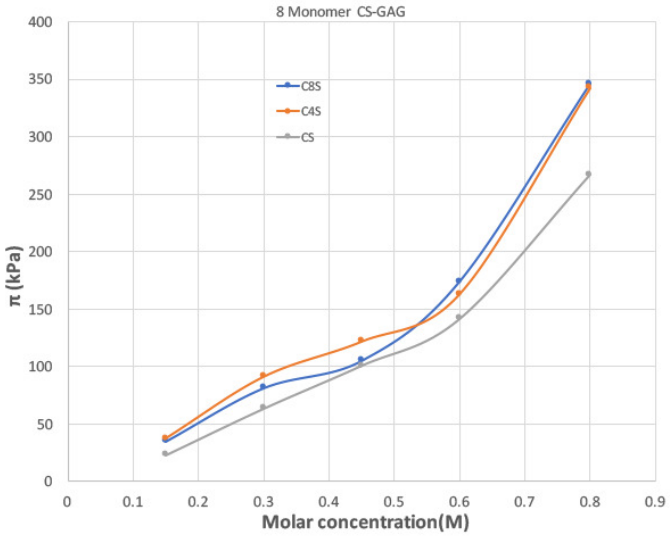

b)

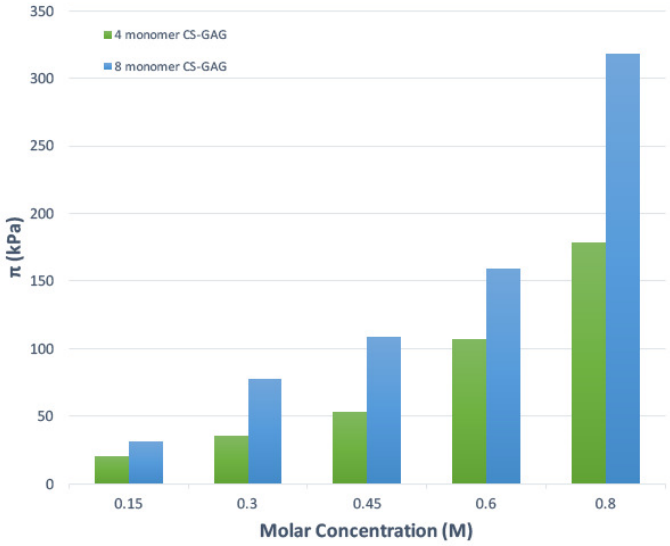

c)